Current Biology, Volume *30*

Supplemental Information

Constrained Structure of Ancient Chinese Poetry Facilitates Speech Content Grouping

Xiangbin Teng, Min Ma, Jinbiao Yang, Stefan Blohm, Qing Cai, and Xing Tian

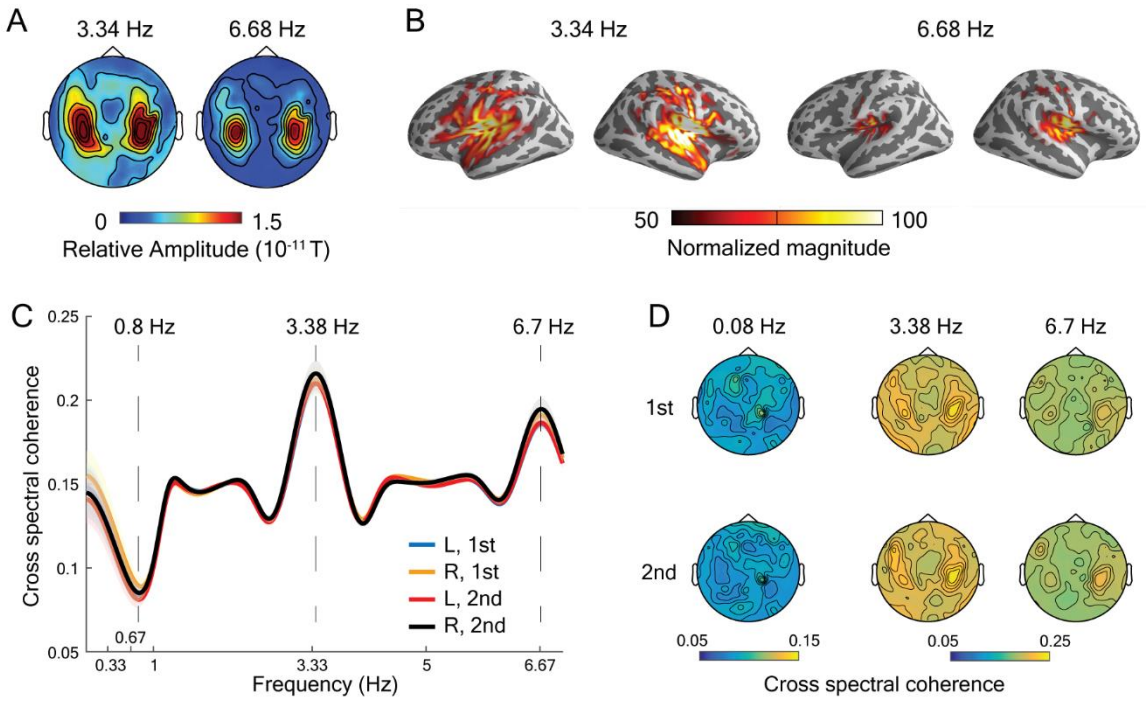

Figure S1. Auditory responses to the poem stimuli and acoustic-neuro coherence, Related to Figure 1&2. (A) MEG topographies of the relative amplitude spectrum at 3.34 Hz (the syllable rate: ~3.33 Hz), and 6.68 Hz (the first harmonic component of the syllable rate: ~6.67 Hz). (B) MEG source localization of the spectral components at 3.34 Hz and 6.68 Hz. The neural components evoked by the amplitude envelopes of the poem stimuli were localized around auditory areas. (C) Spectrum of acoustic-neuro coherence. We calculated cross spectral coherence over the auditory channels between the amplitude envelopes of the poem stimuli and the neural signals. The line color codes for hemispheres and presentations. We observed high coherence values around the syllable rate and its first harmonic component, but not around the line rate (~0.67 Hz), the rhyming rate (~0.33 Hz), or around ~0.24 Hz where a repetition effect was shown. We conducted a cluster-based permutation test and did not find a main effect over hemispheres and presentations from 0.1 Hz to 7 Hz ($p < 0.05$). This finding demonstrates that the acoustic properties of the poem stimuli and the auditory-related responses did not explain our findings on the neural tracking of poetic structures of *Jueju* (Figures 2 and 3). The shaded areas represent one standard error of the mean. (D) Topographies of acoustic-neuro coherence at 0.08 Hz, 3.38 Hz, and 6.7 Hz. We chose 0.08 Hz because we observed a dip of coherence in (C).

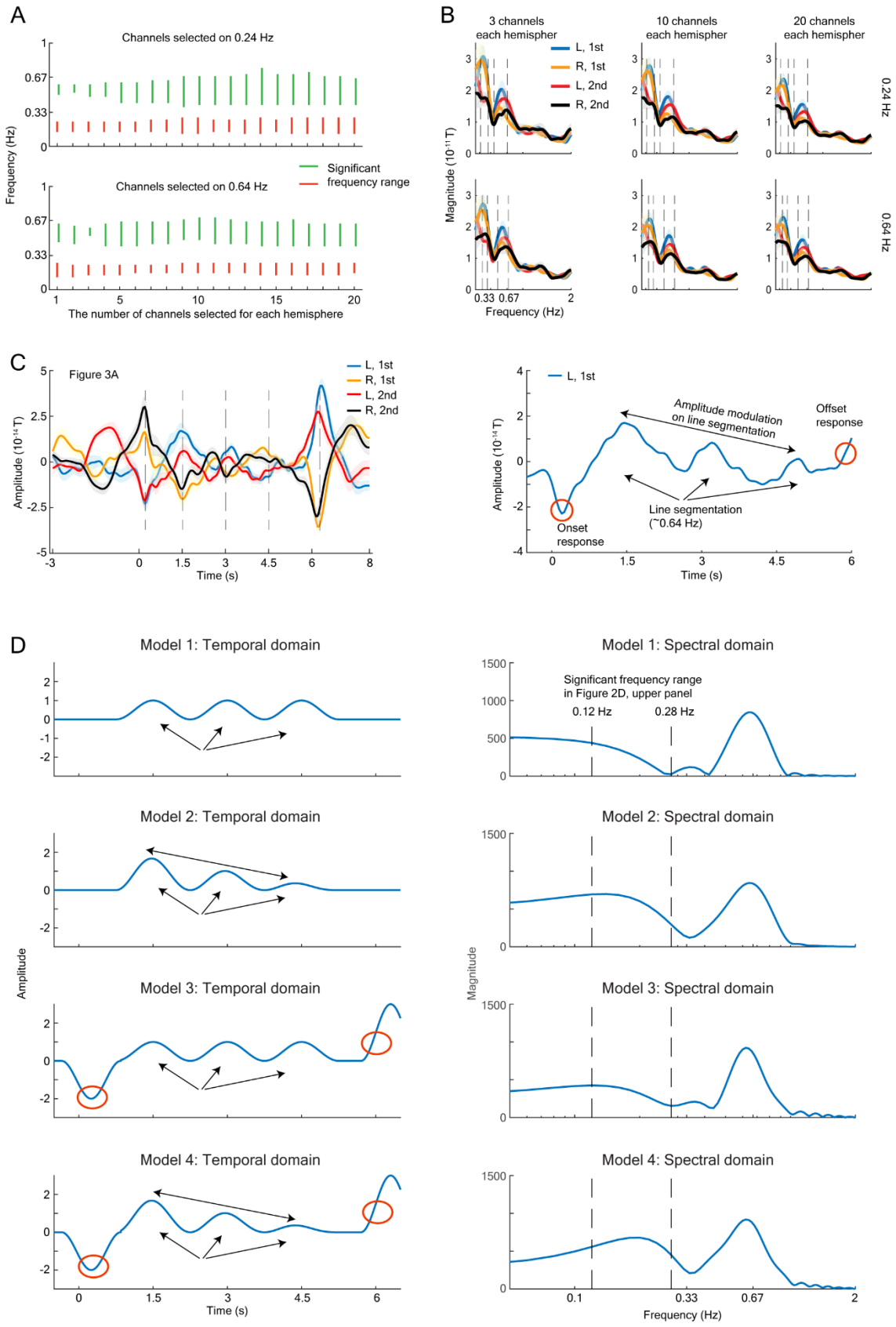
A
Channels selected on 0.24 Hz
Channels selected on 0.64 Hz
Significant
frequency range
Frequency (Hz)
The number of channels selected for each hemisphere
B
3 channels
each hemispher
10 channels
each hemispher
20 channels
each hemispher
L, 1st
R, 1st
L, 2nd
R, 2nd
0.24 Hz
0.64 Hz
Magnitude (10⁻¹¹ T)
Frequency (Hz)
C
Figure 3A
Amplitude (10⁻¹⁴ T)
Time (s)
Amplitude modulation
on line segmentation
Offset
response
Onset
response
Line segmentation
(~0.64 Hz)
D
Model 1: Temporal domain
Model 1: Spectral domain
Significant frequency range
in Figure 2D, upper panel
0.12 Hz
0.28 Hz
Model 2: Temporal domain
Model 2: Spectral domain
Model 3: Temporal domain
Model 3: Spectral domain
Model 4: Temporal domain
Model 4: Spectral domain
Amplitude
Magnitude
Time (s)
Frequency (Hz)

Figure S2. Effect of channel selection on the findings at ~0.64 Hz and ~0.24 Hz and simulation on examining the origin of the effect at ~0.24 Hz, Related to Figure 2&3. (A) We varied the number of the MEG channels included in the analyses to test how the selection affected our findings. The same analysis procedure as in the main text was applied on the data from different numbers of channels. Significant frequency ranges found using data from different number of channels. In Figure 2, we selected 10 MEG channels from each hemisphere based on each of the two frequency component (~0.24 Hz and ~0.64 Hz). Using those selected channels, we further identified the significant frequency range to test lateralization and effects of repetition (Figure 2D). Here, we showed that the similar significant frequency ranges can be found using data from 1 channel to 20 channels. The upper and lower panels show the significant frequency ranges based on the channels selected at ~0.24 Hz and ~0.64 Hz, respectively. This suggests that our findings are robust to the channel selections. (B) Analysis on the channels of interest. The same analysis as in Figure 2D, but with data in different numbers of channels. The profiles of the amplitude spectra did not change regardless of the number of channels used. The amplitude of the spectra decreases with more channels, as a larger number of channels also included those with neural responses of lower magnitude. (C) The left panel is from Figure 3A. On the right, for better visualization, we selected the neural signal from the first presentation and the left hemisphere as an example for demonstration. It can be seen that the temporal range (-0.5 s to 6.5 s) used to calculate the amplitude spectra in Figure 2D included four major components in the neural signals – the onset response, the offset response (both marked by red circles), the neural signals corresponding to the line segmentation (indicated by arrows), and a component of amplitude modulation on the line segmentation (indicated by a double-arrow). One or a few of these four major components probably contributed the effect around the 0.24 Hz. We next constructed simulations to examine the effect of the neural component of ~0.24 Hz. The shaded areas in (B) and (C) represent one standard error of the mean. (D) The panels on the left show the temporal dynamics of each model within the temporal range used for calculating amplitude spectrum. The panels on the right show the corresponding amplitude spectra. The details of model construction can be seen in STAR Methods and the Matlab codes we deposited in OSF. It can be seen that Model 4 included all four components and captured the spectral findings in Figure 2D. The effect around 0.24 Hz came from the change of amplitude modulation on the poetic line segmentation between the first and the second presentations, and that the neural components around 0.24 Hz emerged from a combination of the onset responses to the poem stimuli and the modulation component. We conducted further simulations to validate this observation (STAR Methods).

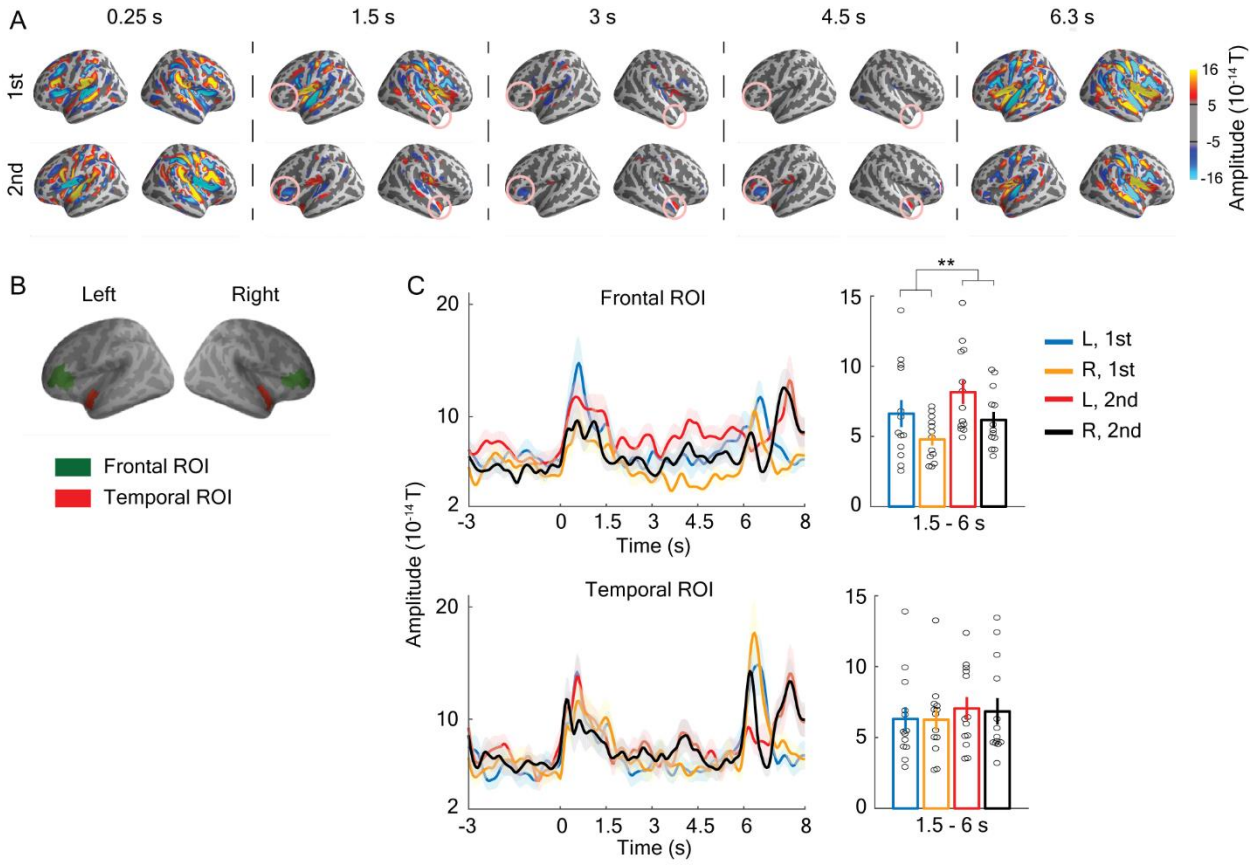

Figure S3. Increased neural activity due to poem repetition in the frontal areas, Related to Figure 3. (A) Source localization of neural dynamics. The peaks in the temporal domain were localized around the auditory and adjacent areas. A decrease in neural activities was observed in the second presentation, which echoes the results of Figure 2D. However, increased neural activities were observed in the left inferior frontal area (around pars triangularis) and the right temporal pole during the second presentation, which were highlighted using pink circles. (B) The corresponding cortical areas in both the left and right hemispheres were selected using a parcellation template as ROIs. (C) ROI analysis. Left, the results of the front ROI. Right, the results of the temporal ROI. It can be seen that the differences of neural activity between the first and the second presentations in the ROIs emerged after the first line, we averaged the neural signals from 1.5 s to 6 s after the onset of the poem stimuli and conducted for each ROI a two-way rmANOVA with the factors of hemisphere and presentation order. In the frontal ROIs, we found a significant main effect of presentation order ($F(1,12) = 11.10$, $p = 0.006$, $\eta_p^2 = 0.481$) (Figure S3C, left panel). The main effect of hemisphere is not significant ($F(1,12) = 4.19$, $p = 0.063$, $\eta_p^2 = 0.259$). The interaction effect is not significant ($F(1,12) = 0.02$, $p = 0.883$, $\eta_p^2 = 0.002$). No significant effects were observed for the temporal ROIs – hemisphere (Fig S3C, right panel): ($F(1,12) = 0.53$, $p = 0.480$, $\eta_p^2 = 0.042$); presentation order: ($F(1,12) = 0.03$, $p = 0.858$, $\eta_p^2 = 0.003$); interaction: ($F(1,12) = 0.02$, $p = 0.892$, $\eta_p^2 = 0.002$). The line color is the same as in Figure S2. The shaded areas represent one standard error of the mean.

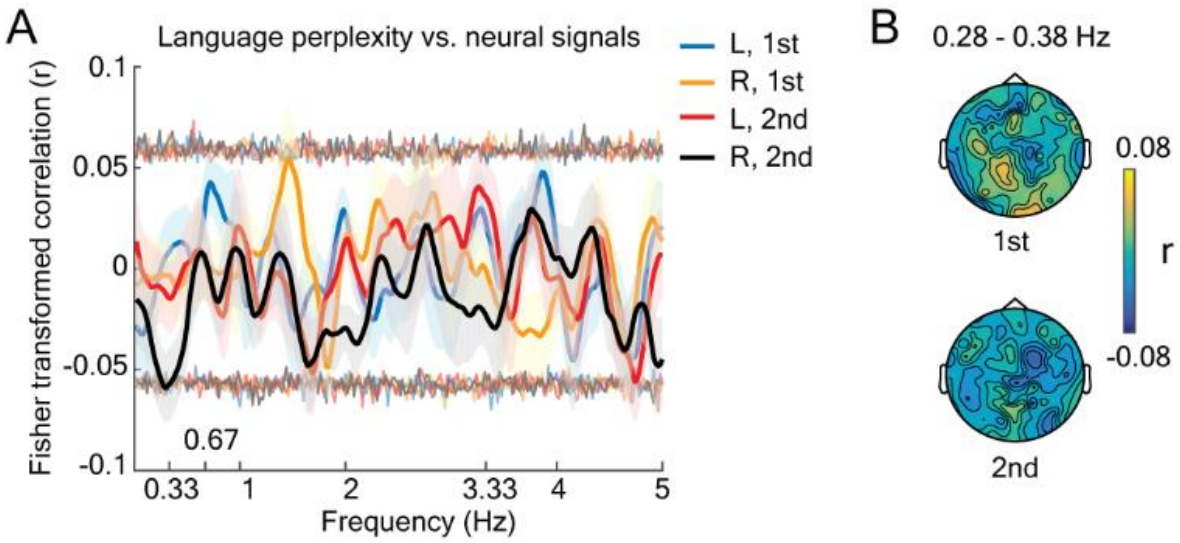

Figure S4. Correlation between language perplexity and speech segmentation at the channels selected at ~0.64 Hz, Related to Figure 4. (A) Language perplexity-neural correlations at the channels selected at ~0.64 Hz. The line color codes hemisphere and presentation. The transparent thin lines (same color code) represent the upper and lower thresholds derived from a permutation test ($p < 0.01$). The shaded areas represent one standard error of the mean. We found significant negative correlations of neural signals of the second representation in the right hemisphere at 0.28 Hz, 0.32 Hz, 0.36 Hz, and 0.38 Hz when we conducted the permutation test at the first time, but the significant correlations were not reliably shown when we conducted the permutation test again. The reason is that the thresholds were derived from the permutation tests and varied to a very small degree every time the permutation test was conducted. In Figure 4B, the significant correlations were always shown in the permutation tests. The lack of test-retest reliability suggests that the finding at 0.28 ~ 0.38 Hz in Figure S4A is not robust, so we did not show this result in the main text nor draw a conclusion from this. Nonetheless, we plotted the topography of the correlations from 0.28 Hz to 0.38 Hz in (B) as in Figure 4C.